Available online at www.sciencedirect.com

SciVerse ScienceDirect

Scripta Materialia 66 (2012) 749–752

Scripta MATERIALIA

www.elsevier.com/locate/scriptamat

On the design of new β-metastable titanium alloys with improved work hardening rate thanks to simultaneous TRIP and TWIP effects

Matthieu Marteleur,[a] Fan Sun,[b] Thierry Gloriant,[c] Philippe Vermaut,[b] Pascal J. Jacques[a,*] and Frédéric Prima[b]

[a] *Université catholique de Louvain, Institute of Mechanics, Materials and Civil Engineering, IMAP, Place Sainte Barbe 2, B-1348 Louvain-la-Neuve, Belgium*

[b] *Laboratoire de Physico-Chimie des surfaces, Groupe de Métallurgie Structurale (UMR 7045), Chimie-ParisTech, 75231 Paris, France*

[c] *Université Européenne de Bretagne, INSA, SCR/Chimie-Métallurgie, UMR CNRS 6226, F-35043 Rennes cedex, France*

Received 28 October 2011; revised 16 January 2012; accepted 25 January 2012
Available online 2 February 2012

In this work, preliminary results are presented on attempts to develop a new family of titanium alloys with high ductility induced by combined transformation-induced plasticity and twinning-induced plasticity effects. Mechanical tests carried out on a binary β-metastable Ti–12 wt.% Mo alloy designed by a formulation strategy based on the "*d*-electron alloy design" show a very high work hardening rate. X-ray diffraction, electron backscattered diffraction and transmission electron microscopy reveal the mechanical activation of twinning and of α′, α″ and ω phases.

Keywords: Titanium alloys (Ti); Stress-induced martensite; Deformation twinning; Large plasticity

As titanium alloys display a unique profile of properties, they are being used increasingly in numerous application fields, ranging from aerospace structures to biomedical devices. Among the recently developed Ti alloys, the β-Ti alloys seem to present a promising combination of mechanical properties. For example, a new generation of β-Ti alloys based on biocompatible alloying elements such as Ta, Nb, Zr and Mo has been designed as low modulus alloys [1] or nickel-free superelastic materials [2,3], mainly for orthopaedic and dental applications as osseointegrated implants. These β-Ti alloys display several reversible or irreversible deformation mechanisms as a function of the β phase stability, such as stress-assisted martensitic phase transformation (β–α″), mechanical twinning and dislocation slip [4,5].

The design strategy of these new Ti alloys has often been based on theoretical prediction tools [6]. Morinaga et al. [7–9] proposed the "*d*-electron alloy design method" to guide the selection of adapted contents of specific alloying elements to bring about the activation of superelasticity. This approach aims to provide a physical background to the phase stability and phase transformations of titanium alloys by connecting the values of two electronic parameters, Bo (the covalent bond strength between Ti and alloying elements) and Md (the mean *d*-orbital energy level concerning electronegativity and elements radius), to the chemical stability of the high-temperature β phase. This model is based on the cluster DV-Xα method [10] for the calculation of these Bo and Md parameters for binary additions. "Alloying vectors" on a Bo/Md map, originating from the Bo and Md values of pure Ti, then represent the ability of each element to stabilize either the α phase or the β phase in binary alloys. Based on this kind of stability map, correlation with superelasticity properties has been established [8], experimentally validating this tool. It was extensively used in the design and optimization of Ti alloys presenting two specific mechanical properties: low apparent modulus and large reversible superelastic deformation.

If β-Ti alloys can now be designed to have adequate elastic properties, this is not yet the case for their plastic behaviour. Indeed, β-Ti alloys for which plasticity is

* Corresponding author. Tel.: +32 10472432; fax: +32 10474028; e-mail: pascal.jacques@uclouvain.be

1359-6462/$ - see front matter © 2012 Acta Materialia Inc. Published by Elsevier Ltd. All rights reserved.
doi:10.1016/j.scriptamat.2012.01.049

driven by dislocation glide present a very low work hardening rate, bringing about rapid strain localization and low ductility levels. This lack of work hardening compared to other body-centred cubic (bcc) materials such as ferritic steels is not thoroughly understood, even though it represents a major drawback for Ti alloys in all kinds of applications requiring plasticity. On the other hand, some Ti alloys can exhibit other deformation mechanisms, namely mechanical twinning or mechanically induced martensitic transformation when the β phase chemical stability decreases. Several studies have reported the activation of $\{3\,3\,2\}\ \langle 1\,1\,3\rangle$ twinning in some metastable β-Ti alloys, resulting in a significant increase in the work hardening rate [11,12], though this increase has not yet been fully explained. On the other hand, the occurrence of twinning is generally accompanied by a small yield stress. Furthermore, the effect of mechanically induced martensitic transformation on the plastic properties of Ti alloys has hardly been investigated and optimized.

The present study aims to show that the alloy design procedure initially developed for superelastic properties of Ti alloys can be extended to their plastic properties, particularly to the prediction of improved work hardening rate, bringing a combination of strength and ductility hardly reported before for Ti alloys. This extension is not straightforward. In order to reach such a combination of properties, another combination of Bo/Md parameters than that initially proposed by Morinaga et al. [8] for superelasticity was selected and tested. The present study confirms the activation of several deformation mechanisms and a large work hardening rate.

Figure 1 corresponds to the region of the *d*-electron alloying map of titanium alloys where the transition between several deformation mechanisms of the β phase is predicted. The design procedure followed here considers that improvements of the work hardening rate could be reached as a result of the activation of several mechanically activated deformation mechanisms (mechanical twinning, stress-induced martensitic transformation and dislocation glide). The alloying vector of Mo is also

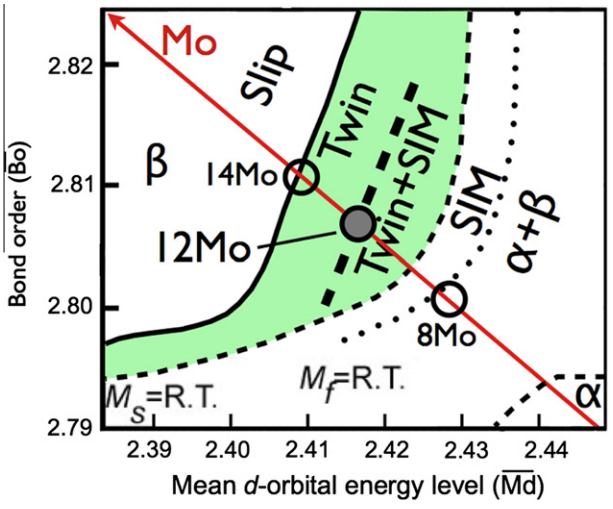

Figure 1. Magnified part of interest of the *d*-electron alloying map for titanium alloys with the alloying vector of molybdenum. The dark linear dashed line indicates the strategic location at which the Ti–12 wt.% Mo alloy is located.

represented in this figure, showing that Mo could be a promising candidate for the development of binary titanium alloys with enlarged plastic properties thanks to the activation of these various deformation mechanisms. Along the alloying vector of Mo, the composition Ti–12 wt.% Mo is located about halfway between the boundaries of the domains of mechanical twinning and stress-induced martensitic transformation. With the values Bo = 2.807 and Md = 2.4158, this alloy was chosen as a good candidate for the improvement of the mechanical properties of as-quenched β phase thanks to expected competition between (mostly) two plastic deformation mechanisms, the transformation-induced plasticity (TRIP) and twinning-induced plasticity (TWIP) effects. It is worth noting that, whereas the Ti–15 wt.% Mo alloy has been extensively studied, hardly any complete study of the microstructure–mechanical properties relationship has been reported in the case of the Ti–12 wt.% Mo alloy. Blackburn and Williams [13] reported the occurrence of mechanical twinning and ω phase in cold rolled samples of Ti–11.6 wt.% Mo. However, they did not measure the mechanical behaviour of these samples. On the other hand, Williams et al. [14] measured the mechanical properties of several Ti–Mo alloys but without any microstructure characterization. More recently, Sun et al. [15] analysed the ageing behaviour of deformed Ti–12 wt.% Mo samples.

The binary Ti–12 wt.% Mo alloy was processed by the cold crucible levitation melting technique under a pure Ar atmosphere. The 20 g ingots produced were then remelted in an arc furnace under a high-purity Ar atmosphere, with a non-consumable tungsten electrode on a water-cooled copper module. The ingots were then cold rolled down to 0.5 mm sheets, corresponding to a reduction level larger than 95%. Cold rolled sheets were reheated under a high vacuum (10^{-7} mbar) up to 1143 K for 30 min for recrystallization and then water quenched to keep the fully β microstructure at room temperature. The resulting grain size was of the order of several tens of microns, while X-ray diffraction showed that this as-quenched microstructure was in a β state, with some athermal ω phase. Great care was taken throughout the processing of the samples to keep the oxygen content as low as possible since it influences the mechanical behaviour. Prior to the mechanical tests, the measured oxygen content was 0.0115 wt.%.

Mechanical properties were measured in tension on specimens with a calibrated gauge length of 24 mm and a width of 4 mm. Specimens deformed to different levels were then observed by electron backscattered diffraction (EBSD) and transmission electron microscopy (TEM). Prior to the EBSD observations, samples were first mechanically polished down to 1 μm and then electropolished using a solution of 53.5% CH_3OH, 33% $C_4H_{10}O$, 11.5% $HClO_4$ and 2% HCl, held at 253 K. EBSD scans were performed using a field emission gun scanning electron microscope operating at 10, 15 or 20 kV, with step sizes ranging from 0.1 to 0.05 μm. A JEOL 2010 field emission gun microscope operating at 200 kV was used. X-ray diffraction measurements (with Cu K_α radiation) were also carried out on these deformed samples in order to highlight the appearance of new phases in the course of plastic straining.

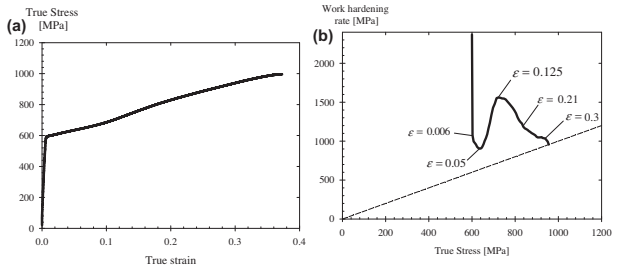

Figure 2. (a) Tensile true stress–true strain curve and (b) evolution of the work hardening rate ($\partial\sigma/\partial\varepsilon$) with the true stress of the investigated Ti–12 wt.% Mo alloy.

Figure 2 presents the tensile true stress–true strain curve, as well as the evolution of the work hardening rate ($\theta=\partial\sigma/\partial\varepsilon$) with stress. The present Ti–Mo alloy exhibits enhanced mechanical properties, particularly a large work hardening rate, bringing about levels of true stress and true strain at necking of 1000 MPa and 0.37, respectively. These values fit with the levels reported by Williams et al. [14], even though their oxygen content was four times higher than in the present study, meaning that this alloy presents a tolerance to the addition of oxygen. The stress–strain curve and, more pronouncedly, the work hardening rate show non-monotonous evolutions. After the elastic–plastic transition, the work hardening rate exhibits a large hump, followed by a smooth decrease down to the point where the Considere criterion is fulfilled. As it will be explained below, these different steps in the work hardening rate evolution are related to the activation of different deformation mechanisms. It should be noted that the maximum work hardening rate is close to the theoretical limit ($\mu/20$) [16].

Figure 3 shows EBSD maps of a specimen deformed to a tensile strain of 0.05. These maps show that, in the Ti–12Mo alloy, the strain is actually accommodated by a combination of several deformation mechanisms. This figure first shows that mechanical twinning is activated well at a strain of 0.05. Two twinning systems forming a regular pattern are observed and indexed as $\{3\,3\,2\}\langle 1\,1\,3\rangle$ twins in the bcc β phase. Observation of the band contrast of the individual twins (Fig. 3(a)) suggests that additional internal deformation mechanisms (twinning and/or mechanically induced α″) occur at the nanoscale, showing that the strain is accommodated at different microstructural scales. Extra characterization is needed to clearly identify these internal features.

Besides mechanical twinning, some features of the deformed microstructure were indexed as hexagonal close-packed α′ phase (represented in red in Fig. 3(a)). The presence of this mechanically induced α′ phase was also confirmed by X-ray diffraction measurements at strain levels as low as 0.02. The mechanical activation of the α′ phase is not common and was not anticipated in the present alloy, even though it has already been reported in some β-metastable Ti alloys [17,18].

Figure 4 shows TEM micrographs of a sample strained to necking ($\varepsilon = 0.38$), illustrating the complex mixture of strain-induced coexisting networks of α″ phase and mechanical twins. Figure 4(a) corresponds to a bright-field (BF) TEM micrograph along the $\langle 1\,1\,3\rangle$ zone axis. The spots corresponding to the α″ phase

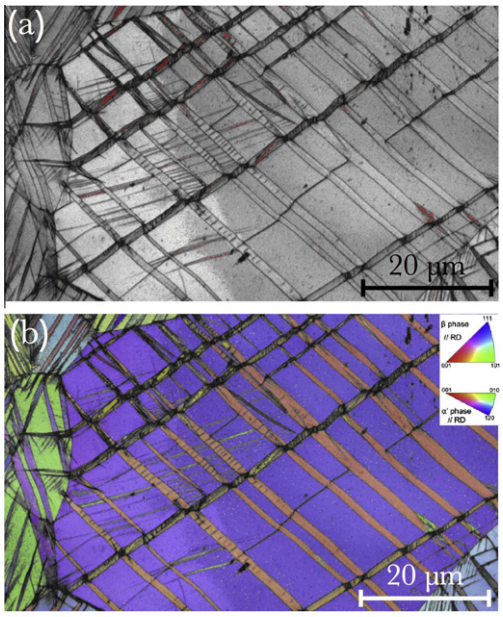

Figure 3. EBSD maps of a specimen deformed to a tensile strain of 0.05. (a) Band contrast map with the α′ phase represented in red; (b) inverse pole figure map for the rolling direction. The indexed α′ bands satisfy the Burgers relationship $\langle 1\,1\,1\rangle_\beta \| \langle 11\text{–}20\rangle_{\alpha'}$ and $\{1\,1\,0\}_\beta \| \{0\,0\,0\,1\}_{\alpha'}$, while $\{3\,3\,2\}\langle 1\,1\,3\rangle$-type mechanical twinning occurs. (For interpretation of the references to colour in this figure legend, the reader is referred to the web version of this article.)

are clearly visible. The formation of this strain-induced orthorhombic α″ phase leads to a dense network of nanoscale needles. The presence of this phase was also detected by X-ray diffraction from as low a strain level as 0.10. On the other hand, Figure 4(b) corresponds to another BF TEM micrograph of a zone close to the lower right corner of Figure 4(a). In this figure, another dense network is visible, corresponding to mechanical twins. A magnified view of these mechanical twins is given on the $\langle 1\,1\,0\rangle_\beta$ HRTEM micrograph of Figure 4(c). This figure confirms the occurrence of the $\{3\,3\,2\}\langle 1\,1\,3\rangle$ mechanical twinning. Furthermore, the power spectra taken on both sides of the twinning plane exhibit the diffracting signature of the ω phase close to the twin boundary. This ω phase formation is believed to happen to accommodate the deformation induced by the twin formation, as already previously reported in association with the $\{3\,3\,2\}\langle 1\,1\,3\rangle$-type twins. This study thus highlights the fact that the enhanced mechanical behaviour of the Ti–12 wt.% Mo alloy relies on a complex combination of several deformation mechanisms, including stress-induced martensitic transformations (from β to α′ and/or α″) and an intense mechanical twinning associated with the formation of the ω phase. The exact chronology regarding the occurrence of the different mechanisms is still not completely understood, especially concerning a possible transition from the β→α′ stress-induced transformation to the more classical β→α″ transformation when the strain level is increased.

As predicted by the *d*-orbital design strategy, the position of the investigated composition on the Bo–Md map seems to result in a competition between stress-induced martensite (β→α′ and β→α″) and mechanical twinning as deformation mechanisms. While the large

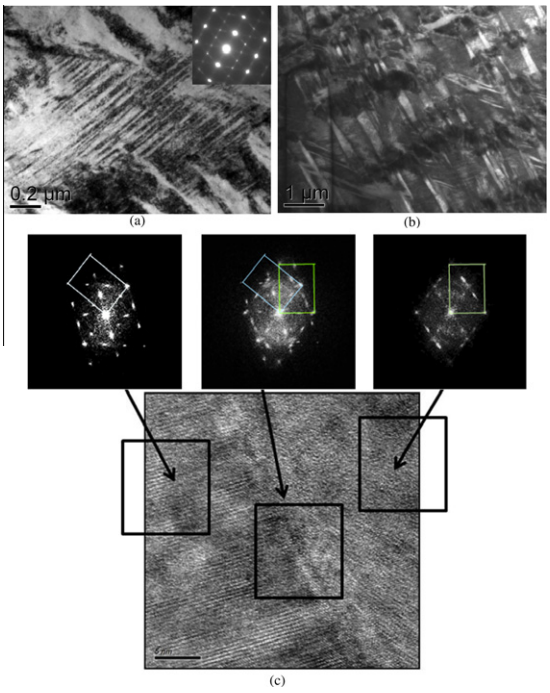

Figure 4. TEM micrographs of a specimen deformed to 0.38. (a) BF micrograph along the $\langle 1\,1\,3\rangle_\beta$ zone axis illustrating the formation of stress-induced α'' martensite; (b) BF micrograph showing the occurrence of intense $\{3\,3\,2\}\ \langle 1\,1\,3\rangle$ mechanical twinning; (c) $\langle 1\,1\,0\rangle_\beta$ high-resolution TEM micrograph of a zone of (b) corresponding to a $\{3\,3\,2\}\ \langle 1\,1\,3\rangle$ mechanical twin boundary. Spots corresponding to the ω phase are also visible on the power spectra.

increase in the work hardening rate seems to depend on the activation of these phenomena, the role of each of them is not yet clearly established. Indeed, the present evolution of the work hardening rate is not usual for bcc titanium alloys. Several analyses have been carried out in other metallic systems, such as advanced steels, in which such deformation mechanisms also occur [19,20]. It was proposed [20,21] that the hardening resulting from mechanical twinning, for example, is related to a decrease in the effective grain size (a so-called dynamic "Hall–Petch" effect) since new, highly misoriented twin boundaries are continuously created, bringing about a decrease in the dislocation mean free path. Additionally, the formation of twins could also induce some kind of composite effect, with twins developing their own mechanical behaviour with respect to the imposed stress. Moreover, the twin boundaries are probably accompanied by the creation of new dislocations on both sides of the boundaries, which will harden the matrix by deforming it. Figure 4(b) also shows that mechanical twinning continues to be activated at larger strains, bringing about complex nanostructured patterns of highly disoriented grains.

It is thought from these results that the successive stress-induced transformations actually participate to the strain hardening behaviour. This is consistent with previous work reporting that β-metastable alloys with stress-induced martensite $\beta\rightarrow\alpha''$ transformation had a higher work hardening rate than corresponding $\alpha+\beta$ alloys, where only dislocation slip is occurring [22].

In summary, several deformation mechanisms have been identified in the present Ti–12 wt.% Mo alloy, i.e. $\{3\,3\,2\}\ \langle 1\,1\,3\rangle$ mechanical twinning and the formation of α', α'' and ω phases. The formation of α' essentially happens at the onset of plasticity, while the other mechanisms are active during the whole plastic straining. Such a complex combination of deformation mechanisms has been hardly reported in the literature [23,24], and this first set of results is promising for the development of a new family of β-metastable Ti alloys exhibiting TRIP/TWIP effects, resulting in a unique combination of strength and ductility. Furthermore, the simultaneous occurrence of these effects suggests that the extension of the *d*-electron alloy design strategy for plastic properties is reasonably valid in binary alloys.

This work was carried out within the framework of the IAP programme.

[1] M. Niinomi, T. Akahori, S. Katsura, K. Yamauchi, M. Ogawa, Mater. Sci. Eng. C 27 (2007) 154.
[2] H.Y. Kim, S. Hashimoto, J.I. Kim, T. Inamura, H. Hosoda, S. Miyazaki, Mater. Sci. Eng. A 417 (2006) 120.
[3] Y.L. Hao, S.J. Li, S.Y. Sun, R. Yang, Mater. Sci. Eng. A 441 (2006) 112.
[4] O.P. Karasevskaya, O.M. Ivasishin, S.L. Semiatin, Yu.V. Matviychuk, Mater. Sci. Eng. A 354 (2003) 121.
[5] S. Hanada, O. Izumi, Metall. Trans. A 17 (1986) 1409.
[6] D. Raabe, B. Sander, M. Friak, D. Ma, J. Neugebauer, Acta Mater. 55 (2007) 4475.
[7] D. Kuroda, M. Niinomi, M. Morinaga, Y. Kato, T. Yashiro, Mater. Sci. Eng. A 243 (1998) 244.
[8] M. Abdel-Hady, K. Hinshita, M. Morinaga, Scr. Mater. 55 (2006) 477.
[9] M. Morinaga, N. Yukawa, T. Maya, K. Sone, H. Adachi, in: P. Lacombe, R. Tricot, G. Béranger (Eds.), Proceedings of the Sixth World Conference on Titanium, Paris, Les Editions de Physique, 1988, p. 1601.
[10] M. Morinaga, Y. Murata, H. Yukawa, Hartree–Fock–Slater Method for Materials Science, Springer, Berlin, 2006, p. 23.
[11] S. Hanada, T. Yoshio, O. Izumi, Trans. Jpn. Inst. Met. 27 (1986) 496.
[12] X.H. Min, K. Tsuzaki, S. Emura, K. Tsuchiya, Mater. Sci. Eng. A 528 (2011) 4569.
[13] M.J. Blackburn, J.C. Williams, Trans. Metall. Soc. AIME 242 (1968) 2461.
[14] D.N. Williams, R.A. Wood, E.S. Bartlett, Metall. Trans. 3 (1972) 1529.
[15] F. Sun, F. Prima, T. Gloriant, Mater. Sci. Eng. A 527 (2010) 4262.
[16] U.F. Kocks, H. Mecking, Prog. Mater. Sci. 48 (2003) 171.
[17] M.K. Koul, J.F. Breedis, Acta Metall. 18 (1970) 579.
[18] X. Zhao, M. Niinomi, M. Nakai, J. Mech. Behav. Biomed. (2011), doi:10.1016/j.jmbbm.2011.06.020.
[19] P.J. Jacques, Q. Furnemont, F. Lani, T. Pardoen, F. Delannay, Acta. Mater. 55 (2007) 3681.
[20] H. Idrissi, K. Renard, L. Ryelandt, D. Schryvers, P.J. Jacques, Acta. Mater. 58 (2010) 2464.
[21] O. Bouaziz, S. Allain, C. Scott, Scr. Mater. 58 (2008) 484.
[22] T. Grosdidier, M.J. Philippe, Mater. Sci. Eng. A 291 (2000) 218.
[23] R.J. Talling, R.J. Dashwood, M. Jackson, D. Dye, Acta Mater. 57 (2009) 1188.
[24] Y. Yang, G.P. Li, G.M. Cheng, H. Wang, M. Zang, F. Xu, K. Yang, Scr. Mater. 58 (2008) 9.